

## Physiology and metabolism of tissue-engineered skeletal muscle

Cindy S Cheng, Brittany NJ Davis, Lauran Madden, Nenad Bursac and George A Truskey

Department of Biomedical Engineering, Duke University, Durham, NC 27708, USA

Corresponding author: George A Truskey. Email: george.truskey@duke.edu

### Abstract

Skeletal muscle is a major target for tissue engineering, given its relative size in the body, fraction of cardiac output that passes through muscle beds, as well as its key role in energy metabolism and diabetes, and the need for therapies for muscle diseases such as muscular dystrophy and sarcopenia. To date, most studies with tissue-engineered skeletal muscle have utilized murine and rat cell sources. On the other hand, successful engineering of functional human muscle would enable different applications including improved methods for preclinical testing of drugs and therapies. Some of the requirements for engineering functional skeletal muscle include expression of adult forms of muscle proteins, comparable contractile forces to those produced by native muscle, and physiological force–length and force–frequency relations. This review discusses the various strategies and challenges associated with these requirements, specific applications with cultured human myoblasts, and future directions.

**Keywords:** Myoblast, skeletal muscle myotube, tissue engineering, contractile force, bioreactors

*Experimental Biology and Medicine* 2014; 239: 1203–1214. DOI: 10.1177/1535370214538589

### Introduction

Tissue engineering of functional human skeletal muscle can lead to new treatments of injured and diseased muscle and development of high fidelity systems to study muscle function in response to drugs and toxins *in vitro*. One of the key challenges in skeletal muscle tissue engineering is to re-create the proper structural organization of the native muscle to ensure the most efficient generation and transmission of contractile force. Specifically, native muscle is composed of multinucleated fibers that are less than 100  $\mu\text{m}$  in diameter which often span the entire muscle length. Each myofiber contains thousands of myofilaments consisting of repeating functional units known as sarcomeres (Figure 1(a)) that produce the striated appearance of skeletal myofibers. Sarcomeres consist of alternating actin (thin) and myosin (thick) filaments with thin filaments being connected to Z lines, which delineate the borders of the sarcomere. Sarcomeres are surrounded by the sarcoplasmic reticulum network which stores and releases calcium ions during contraction. The force of contraction is directly determined by the length of sarcomere (Figure 1(b)). Via the dystrophin-associated protein complex, individual myofibers are attached to a thin layer of connective tissue called endomysium.<sup>4</sup> Groups of myofibers form fascicles, which are surrounded by a connective tissue layer called perimysium that harbors blood vessels and nerves, and multiple fascicles form the muscle that at its ends is attached to bone

via tendons. This interconnection of muscle cells and matrix enables the entire muscle to contract in a coordinated fashion.

Most of the *in vitro* engineered three-dimensional (3D) skeletal muscle tissues possess many of the important features of native muscle fascicle, while lacking higher-order structures including multifascicle organization, tendons, and the neurovascular bed. Specifically, engineered muscles exhibit key functional proteins found in mature muscle, including abundant cross-striations (Figure 1(c)), myotendinous-like junctions (Figure 1(d)), contraction in response to electrical/neural stimuli, and force–length and force–frequency relationships qualitatively similar to those of excised myofibers.<sup>5</sup> However, engineered muscles also exhibit lower specific forces than those found *in vivo*,<sup>6</sup> smaller diameters of muscle fibers, immature forms of muscle proteins,<sup>7</sup> alterations in the abundance and distribution of glucose transporters,<sup>8</sup> and dominance of anaerobic glycolysis rather than oxidative phosphorylation.<sup>8</sup> All of these differences between muscle fibers *in vitro* and *in vivo* affect the function of engineered muscle *in vitro*.

In this review, we first discuss factors that influence the development of engineered muscle. We then examine strategies to stimulate myofiber maturation, including microRNA modulation of protein expression and innervation by co-culture. We conclude with a summary of challenges that need to be addressed to promote engineering of differentiated and functional human muscle fibers *in vitro*.

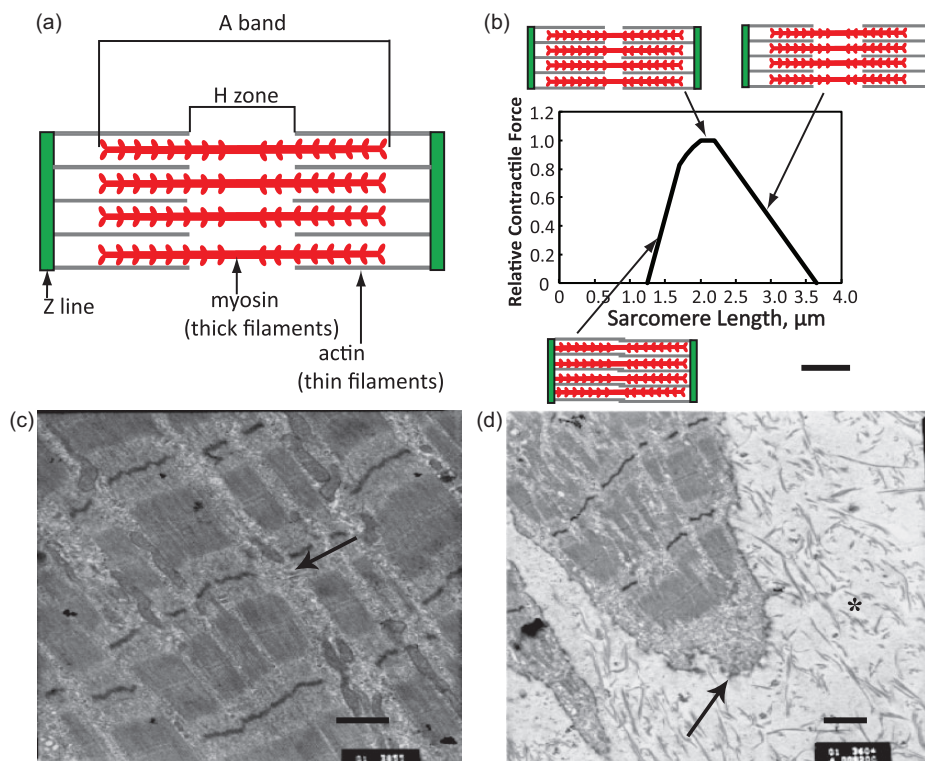


**Figure 1** Sarcomere structure during contraction (a) Schematic of the components of the sarcomere as seen by electron microscopy (A band, Z line, H zone, and thin and thick filaments) and relative location of actin and myosin. (b) Force–length relationship for the sarcomere and change in sarcomere structure with sarcomere length. Adapted from Hall<sup>1</sup> and Krans.<sup>2</sup> (c) Electron micrograph of three-dimensional mouse C2C12 myotubes in collagen gel for 16 days. Mature sarcomeres are evident as well as T-tubules (arrow), from Rhim et al.<sup>3</sup> with permission. (d) Shown at the end of a myofiber is a newly forming myotendinous junction (arrow), which exhibits terminal, invaginated ends. Collagen I fibers show the 64-nm periodic banding pattern characteristic of mature myofibrils and are dispersed at the ends (\*). Scale bars, 1  $\mu\text{m}$ . From Rhim et al.<sup>3</sup> with permission. (A color version of this figure is available in the online journal.)

## Factors affecting the formation of engineered muscle

Optimized culture conditions to efficiently expand human myoblasts and promote their fusion and maturation are influenced by the cell source, methods to prepare 3D constructs, application of electrical or mechanical stimulation, oxygen transport, metabolism, and the presence of particular skeletal myofiber types.

### Cell sources for muscle tissue engineering

The most utilized source for muscle tissue engineering is the putative muscle stem cell, the satellite cell. Satellite cells reside in their niches between the myofiber plasma membrane and basal lamina<sup>9–11</sup> and express the transcription factor Pax7, which is important for self-renewal. Under normal conditions, satellite cells remain quiescent in the periphery of the myofiber with limited gene expression and protein synthesis.<sup>9</sup> In response to muscle injury or trauma, growth factors and cytokines released from damaged myofibers signal satellite cells to leave their niche and begin to proliferate, co-express Pax7 and MyoD, and undergo myogenic commitment.<sup>9</sup> As activated satellite cells proliferate, they downregulate Pax7 and upregulate the myogenic transcription factors MyoD to become myoblasts which in turn upregulate myogenin. Myoblasts then begin to fuse to form new myotubes.<sup>9–11</sup> *In vivo*, some

myoblasts maintain their Pax7 expression and lose their myogenic marker expression to ultimately leave the cell cycle and return to a quiescent state. The renewed satellite cell pool, if activated, can re-enter a new cycle of repair and regeneration.<sup>9</sup> While satellite cell commitment to myoblasts and myotube fusion has been shown in cell culture, establishment of natural satellite cell niches and self-regenerative capacity of engineered muscle are still to be demonstrated *in vitro* and *in vivo*.

As shown in numerous studies, satellite cells can be readily isolated from muscle biopsies of animals and humans to produce skeletal myoblasts *in vitro*. Like primary rodent myoblasts and various cell lines, human myoblasts derived from satellite cells form differentiated myofibers with characteristic sarcomeric striations and express myosin heavy chain (MHC), MyoD, and desmin.<sup>12,13</sup> Differentiation of human muscle cells to form mature myotubes is slower than for mouse or rat muscle cells and the media requirements are more stringent.<sup>14</sup> For engineered 3D human skeletal muscle, desmin positive myoblasts should be at least 75% of the cell population to successfully produce cross-striated myotubes *in vitro*.<sup>12</sup>

To inhibit further proliferation and promote myoblast differentiation and fusion, the media is switched to low growth factor serum culture medium or serum-free medium. In 3D skeletal muscle cultures, a high density of myoblasts is needed for fusion and enough muscle fibers

are needed to form in parallel to exert significant contractile forces along the fiber direction. This necessitates expanding myoblasts sufficiently while ensuring that the cells still differentiate into functional myofibers. Interestingly, not all myoblasts in culture fuse to form fibers and the extent of myofiber formation declines with continued subculture.<sup>15</sup> To counter this decline and form high-density myofiber cultures, forskolin, which activates cyclic adenosine monophosphate, could be added to promote myoblast proliferation without compromising the ability to form myotubes.<sup>16</sup>

Other subpopulations of muscle stem cells can form myofibers but these stem cells are rare and/or multipotent.<sup>17</sup> For example, human muscle-derived progenitor cells isolated by Huard and co-workers<sup>19</sup> can differentiate into skeletal muscle cells, cardiomyocytes, endothelial cells, pericytes, chondrocytes, and bone cells. A fraction of these cells with elevated levels of aldehyde dehydrogenase resists oxidative stress and exhibits increased proliferation and ability to form myotubes,<sup>20</sup> suggesting a promising cell source for muscle tissue engineering. Embryonic stem cells and induced pluripotent stem cells are another cell source that can differentiate into muscle cells and hold the promise of providing a ready source of satellite cells and myoblasts,<sup>21–23</sup> but further work is needed to produce sufficient numbers of cells to generate contractile myofibers, and address potential safety concerns.<sup>17</sup>

### Methods to form 3D engineered muscle

Engineered 3D skeletal muscle has been produced in the form of scaffold-free muscle bundles (myooids)<sup>5</sup> or by embedding myogenic cells into non-biodegradable or biodegradable hydrogels and polymer scaffolds.<sup>3,24–26</sup>

Myooids are formed from contracting sheets of myofibers. Fibroblasts are essential for myooids to form, synthesizing the extracellular matrix needed for structural support.<sup>6</sup> After two weeks of culturing myooids, myotubes occupy 30–60% of the total myooid cross-sectional area with fibroblasts and extracellular matrix occupying the rest. However, myofibers in myooids lack the uniform alignment present in adult mammalian skeletal muscle, are rarely cross-striated, and mostly contain centrally located nuclei, a sign of muscle immaturity.<sup>5</sup>

Myooids take over one month to produce,<sup>27</sup> whereas relatively mature 3D engineered fibrin hydrogel muscle bundles can be produced in 10–12 days.<sup>5,28</sup> Engineered muscle bundles made with collagen or fibrin hydrogels can survive for about 42 days without electrical or mechanical stimulation,<sup>27</sup> while myooids prepared with primary myoblasts and fibroblasts and without a hydrogel can survive as long as 100 days.<sup>5</sup>

Organized, aligned myofibers in culture can be formed by micropatterning or generating tension by fixing the ends of engineered constructs and allowing contraction of the cells.<sup>29</sup> Other methods to establish a more mature myofiber phenotype include incorporating specific peptide sequences of extracellular matrix proteins or signaling molecules in the scaffold,<sup>30</sup> or application of electrical or mechanical stimulation.<sup>31</sup>

Engineered skeletal muscle bundles in hydrogels have been produced using fibrin, Matrigel, hyaluron, or collagen-based hydrogels.<sup>3,25,28,32</sup> Collagen hydrogels are stiffer and tend to rupture more easily at high cell densities which limit the contractile forces that can be studied.<sup>5,28</sup> Fibrin gels assemble into a network of branching fibers,<sup>33</sup> enabling them to withstand higher contractile forces and better support spontaneous twitching of myofibers. Adjusting the concentration of aminocaproic acid (ACA) in the differentiation media inhibits rapid fibrin gel degradation by serum plasma.<sup>28</sup> The rigidity of a surrounding matrix also influences myoblast fusion and differentiation. For example, myoblast differentiation is enhanced on protein coated polyacrylamide hydrogel surfaces with elastic moduli of 8–12 kPa,<sup>34</sup> which modulates integrin engagement with the cytoskeleton.<sup>35</sup> The optimal hydrogel stiffness for muscle formation in a 3D environment has not been yet determined and, similar to 2D substrates, may vary with the hydrogel type and cross-linking density as well as the cell-mediated re-modeling process.<sup>36,37</sup>

### Metabolism and myofiber types

Under resting conditions, skeletal muscle energy needs are met by fatty acid breakdown. Muscle has limited permeability to glucose due to low levels of the primary glucose transporter, GLUT4. GLUT4 resides on intracellular vesicles and transport to the plasma membrane is increased by elevated plasma insulin levels<sup>38</sup> enabling glucose to enter myofibers. Glucose is stored as glycogen to meet long-term energy needs, and fatty acid metabolism is reduced. Moderate to heavy exercise causes GLUT4 translocation to the cell membrane independent of insulin, thereby increasing glucose uptake.<sup>39</sup> In culture, GLUT4 surface expression is low and the GLUT1:GLUT4 ratio is higher than *in vivo*,<sup>15</sup> possibly resulting from the denervated state of cultured myotubes.

To meet varied energy demands, skeletal muscle contains slow (Type I) and fast (Type II) twitch fibers, defined in terms of their contraction speed.<sup>40</sup> Human myofiber types are defined, in part, by expression of the contractile protein MHC which has adult (I, IIA, IIB, IIX), embryonic (III), and neonatal isoforms (8).<sup>41</sup> During postnatal development, MHC gene expression transitions from embryonic (MHC III), to postnatal (MHC 8) to adult isoforms.<sup>42</sup> Individual myofibers consist of one or two isoforms.<sup>43</sup> The speed of muscle contraction is dependent on the MHC isoform.<sup>44</sup>

Type I fibers utilize oxidative metabolism, are rich in mitochondria and myoglobin, and sustain aerobic activity using fats and carbohydrates as fuel (Table 1).<sup>41</sup> Slow myosin cross-bridge cycling and a combination of both low abundance and activity of energy-consuming calcium pumps in the sarcoplasmic reticulum reduce the energy demands of Type I fibers.<sup>60</sup> In contrast, rapid cross-bridge cycling and significant calcium fluxes are hallmarks in the fast twitch Type II fibers, resulting in much higher energy demands.<sup>60</sup>

Although MHC isoforms expressed by myotubes derived from rodent myoblasts reflect the distribution

**Table 1** Functional differences between native versus tissue-engineered fibers

| Native fibers                            |                                 |     | Tissue-engineered fibers |  |     |
|--|---------------------------------|-----|--------------------------|--|-----|
| Value                                    | Muscle                          | Ref | Value                    | Cell type                                    | Ref |
| <i>Muscle fiber type</i>                 |                                 |     |                          |  |     |
| Type I: 50%                              | Human vastus lateralis          | 45  | Type I: 10%              | Primary mouse myoblasts                      | 46  |
| Type IIa: 38%                            |                                 |     | Type IIa: 0%             |  |     |
| Type IIb: 12%*                           |                                 |     | Type IIb: 10%            |  |     |
|  |                                 |     | Type IIc: 26%            |  |     |
|  |                                 |     | Embryonic: 44%           |  |     |
|  |                                 |     | Perinatal: 8%*           |  |     |
| Type I: 48.7 ± 0.9                       | Human vastus lateralis          | 47  | Type I: 56%              | Human muscle-derived cells                   | 12  |
| Type I/IIa: 0.1 ± 0.1                    |                                 |     | Type IIa: 0%             |  |     |
| Type IIa: 42.2 ± 1.6                     |                                 |     | Type IIx: 5%             |  |     |
| Type IIax: 2.8 ± 0.5                     |                                 |     | Embryonic: 11%           |  |     |
| Type IIcx: 6.2 ± 1.6 <sup>†</sup>        |                                 |     | Perinatal: 28%*          |  |     |
| Type I: 52.3 ± 3.2                       | Rat vastus intermedius          | 47  | Type I: 75%              | Mouse primary myoblast                       | 31  |
| Type I/IIa: 2.1 ± 0.7                    |                                 |     | Type IIa: 1%             |  |     |
| Type IIa: 41.3 ± 2.2                     |                                 |     | Type IIb: 11%            |  |     |
| Type IIax: 1.2 ± 0.2                     |                                 |     | Perinatal: 13%*          |  |     |
| Type IIcx: 2.8 ± 0.8                     |                                 |     |                          |  |     |
| Type IIcx: 0.3 ± 0.2 <sup>†</sup>        |                                 |     |                          |  |     |
| Type I: 2.4 ± 0.5                        | Mouse vastus intermedius        | 47  | Type I: 68%              | C <sub>2</sub> C <sub>12</sub> cell line     | 31  |
| Type I/IIa: 0.3 ± 0.2                    |                                 |     | Type IIa: 1%             |  |     |
| Type IIa: 37.6 ± 3.2                     |                                 |     | Type IIb: 14%            |  |     |
| Type IIax: 9.4 ± 0.6                     |                                 |     | Perinatal: 17%*          |  |     |
| Type IIcx: 24.7 ± 1.3                    |                                 |     |                          |  |     |
| Type IIcx: 2.1 ± 0.5                     |                                 |     |                          |  |     |
| Type IIb: 23.5 ± 2.5 <sup>†</sup>        |                                 |     |                          |  |     |
| <i>Tetanus to twitch ratio</i>           |                                 |     |                          |  |     |
| 6.25 ± 3.13                              | Rat soleus                      | 48  | 2.11 ± 0.25              | Rat neonatal primary myoblasts               | 28  |
| 9.09 ± 0.83                              | Rat sternohyoid                 | 49  | 2.45 ± 0.28              | Rat primary myoblasts                        | 27  |
| 7.14 ± 1.53                              | Rat extensor digitorum longus   |     |                          |  |     |
|  | Rat gastrocnemius               | 50  | 2.15 ± 0.40              | Mouse primary myoblasts                      | 51  |
| 5.26 ± 1.94                              | Type IIA                        |     |                          |  |     |
| 4.93 ± 1.45                              | Type IIX                        |     |                          |  |     |
| 7.19 ± 2.59                              | Type I                          |     |                          |  |     |
| 10.6 ± 6.1                               | Human first dorsal interosseous | 52  | ~4                       | Primary mouse myoblasts                      | 53  |
| <i>Specific force (kN/m<sup>2</sup>)</i> |                                 |     |                          |  |     |
| 155 ± 13 <sup>‡</sup>                    | Human tibialis anterior         | 54  | 36.3                     | Primary rat myoblast                         | 55  |
| 150 ± 12 <sup>‡</sup>                    | Human soleus                    | 54  | 2.9                      | Primary rat myoblasts                        | 5   |
| 235 ± 6 <sup>†</sup>                     | Mouse extensor digitorum longus | 56  | 0.893 ± 0.110            | Primary mouse myoblasts                      | 53  |
| 259 ± 18 <sup>‡</sup>                    | 259 ± 18 <sup>‡</sup>           | 57  | 19.2                     | C <sub>2</sub> C <sub>12</sub> + fibroblasts | 58  |
|  |                                 |     | 0.9 ± 3.6*               | Avian myoblasts                              | 59  |

\*Value estimated from figure.

<sup>‡</sup>Mean ± SD.<sup>†</sup>Mean ± SE.

found in the muscle from which the cells are derived, cultured human myotubes express MHC IIX, MHC IIA, and MHCI in ratios that differ from those found in the muscle of origin.<sup>15</sup> Limited studies with human myoblasts have shown that after seven days, embryonic (MYH3), perinatal (MYH8), Type I (MYH7), Type IIA (MYH2), and Type IIB (MYH1) mRNA are expressed.<sup>12</sup> After three weeks, adult MHC I was the major isoform,<sup>12</sup> suggesting maturation of myofibers *in vitro*. Overall, compared to adult native muscle, myotubes *in vitro* express significantly larger

fractions of embryonic and perinatal isoforms of MHC (Table 1). Such immature forms of contractile proteins limit the function of the engineered muscle.

Type I and II fibers differ by size and primary means of adenosine triphosphate (ATP) synthesis. Type I slow oxidative fibers rely on oxidative metabolism and are generally smaller in diameter than Type II fibers, which are used for fast, powerful movement.<sup>61</sup> Fibers utilizing anaerobic glycolysis fatigue quickly, due to the limited amount of glucose or glycogen accessible within muscle. In contrast, aerobic

**Table 2** Oxygen consumption rates of muscle

| Resting OCR  | Exercise OCR             | Measurement anatomy or cell type                              | Reference |
|--|--------------------------|---|-----------|
| <i>In vivo</i> consumption rates, nmol O <sub>2</sub> /cm <sup>3</sup> /s  |                          |   |           |
| 0.82 ± 0.23*   | 4.31 ± 2.01*             | Forearm flexor muscle of healthy adults                       | 62        |
| 0.77 ± 0.22*   | 4.15 ± 1.87*             | Forearm flexor muscle of healthy adults                       | 63        |
| 0.26 ± 0.02 <sup>†</sup>   | 1.12 ± 0.11 <sup>†</sup> | Forearm flexor muscle of healthy adults                       | 64        |
| 1.79 ± 0.52*   | n/a                      | Forearm flexor muscle of healthy adults                       | 65        |
| 0.87 ± 0.24 <sup>†</sup>   | 4.5 ± 1.0 <sup>†</sup>   | Forearm flexor muscle of healthy adults                       | 66        |
| 5.82 ± 0.65  | 275 ± 33                 | Vastus lateralis muscles and rectus femoris of healthy adults | 67        |
| <i>In vitro</i> consumption rates, nmol O <sub>2</sub> /cm <sup>3</sup> /s |                          |   |           |
| 6.27   | n/a                      | C2C12 myoblasts   | 68        |
| 0.11   | n/a                      | C2C12 myoblasts in suspension                                 | 69        |
| 8.87 ± 0.05  | n/a                      | Differentiated C2C12 myotubes                                 | 70        |
| 0.128 ± 0.003  | n/a                      | C2C12 myoblasts   | 71        |
| 0.12   | n/a                      | Differentiated C2C12 myotubes                                 | 72        |

\*Mean ± SD.

<sup>†</sup>Mean ± SE.

n/a: not available.

metabolism depends upon the more abundant glucose and fatty acids in blood. Although oxidative phosphorylation is a slower process (1 mole of ATP per min versus 2.5 moles of ATP per minute for anaerobic glycolysis.<sup>1</sup>), ATP synthesis is significantly more efficient; 36 molecules of ATP are produced per molecule of glucose, as opposed to the 2 molecules of ATP per glucose produced during anaerobic glycolysis.<sup>1</sup> *In vitro*, myotube metabolism is primarily anaerobic glycolysis due to the abundance of glucose and poor development of mitochondria.<sup>15</sup>

### Oxygen transport

*In vivo*, skeletal muscle exhibits a range of values for oxygen consumption due to fiber type and metabolic activity (Table 2). On a per cell volume basis, oxygen consumption rates by skeletal myoblasts and myotubes *in vitro* under resting conditions are similar to those of fibers measured *in vivo* (Table 2).

The success of any tissue-engineered construct depends upon the adequate delivery of oxygen to resident cells. The leading limitations to oxygen transport are the physical manner by which it is delivered to the construct and the concentration of dissolved oxygen available. More specifically, transport within the construct scaffold is mainly limited by diffusion and the low dissolved oxygen concentration in the surrounding media.<sup>73</sup> *In vivo*, to meet the high oxygen demand, one or more capillaries surround each myofiber. *In vitro*, the decreased oxygen solubility in media reduces the amount of oxygen in solution and the rate of oxygen delivery, which limits the size and function of developing 3D engineered muscle bundles.<sup>74</sup>

When designing size and function of the muscle bundles, the rate of oxygen delivery to the muscle must equal or exceed the rate of oxygen uptake by muscle. Due to the high oxygen consumption by myotubes and low rate of oxygen delivery,<sup>74</sup> oxygen gradients may be induced in the culture media unless there is mixing in the liquid.

These oxygen gradients result in a high cell density in the peripheral region of the construct surrounding the interior with a lower cell density due to lack of adequate diffusion.<sup>75,76</sup> This leads to a decrease in overall cell density and a heterogeneous density throughout. The steepness of the gradients depend on scaffold structure and porosity, cell type and cell density.<sup>74</sup>

Tissues *in vivo* are exposed to a much lower oxygen concentration than that in which cells are typically cultured *in vitro*.<sup>77,78</sup> Not surprisingly, decreasing oxygen concentration *in vitro* to a more physiological level (1–6% O<sub>2</sub>) enhances myoblast growth and myogenesis.<sup>79–83</sup> Similar results have been obtained in 3D cultures where human myogenic satellite cells cultured under 2% O<sub>2</sub> displayed enhanced proliferation compared to cells cultured under typical culture conditions (21%).<sup>84</sup> Further decrease in oxygen levels (<1% O<sub>2</sub>) tends to inhibit myoblast differentiation.<sup>85</sup>

Oxygen gradients in 3D engineered muscle bundles can be reduced by decreasing its thickness or by increasing oxygen delivery by perfusion,<sup>86</sup> mixing of the fluid, or addition of a perfluorocarbon.<sup>87</sup> Adequate mass transfer could result in an increase in cell density and better uniformity in the packing of bundle layers. For example, dense skeletal muscle bundles were prepared by over-expression of B cell lymphoma 2 (Bcl-2) which inhibits apoptosis arising from nutrient depletion or hypoxia.<sup>88</sup> Bcl-2 over-expression enhanced contractile force generation compared to constructs in which untreated cells inhabited the outer layer of the tissue construct.<sup>88</sup> Additionally, culture in perfluorocarbon elevated the oxygen concentration in solution resulting in increased glucose consumption, lactate production, and generation of contractile forces.

Developing a capillary network within engineered muscle *in vitro*, while likely not beneficial for enhancing the transport of nutrients to cells, can enable rapid

inosculation with host vasculature after implantation and enhance the survival and the development of thicker tissues.<sup>89,90</sup> Microvascular networks can form in a wide range of biodegradable hydrogels,<sup>90</sup> and can be further stabilized by the addition of stromal cells such as embryonic fibroblasts<sup>91</sup> or mesenchymal stem cells.<sup>92</sup> Additionally, alternating layers of skeletal muscle and endothelium produced by cell sheet engineering can yield a 3D network of vessels and myofibers.<sup>93</sup>

### Contractile force generation

The molecular basis for muscle contraction is described by the sliding filament theory.<sup>2</sup> The process begins when acetylcholine released by nerve endings at the neuromuscular junction triggers the influx of calcium ions into the myofiber which induces release of additional calcium ions from the sarcoplasmic reticulum into cytoplasm. Once bound to calcium ions, troponin undergoes a conformational change allowing the myosin head group to bind to the active site on actin and initiate power stroke.<sup>1</sup> In cases of denervated engineered muscles, membrane potential can be depolarized by exogenous electrical stimulus or a bolus of potassium chloride leading to opening of L-type  $\text{Ca}^{2+}$  channels,  $\text{Ca}^{2+}$  transient, and contraction. Most reports of force measurements in engineered muscle employ electrical stimulation at fixed muscle length (isometric conditions) to derive force-length and force-frequency relations.<sup>6,28,51,94</sup> The passive (viscoelastic) and active (contractile) force-length relationships in engineered muscle resemble those of native muscle (Figure 2(a) and (b)), with exception that the ratio of maximum active force to corresponding passive tension is significantly lower in engineered than in native muscle, mostly due to lack of adequate active response.

When a myofiber is stimulated again before returning to the resting length, the intracellular calcium concentration increases and force becomes greater than for a single isolated stimulus. The contractile force increases with frequency of simulation and at 20–100 Hz, depending on the

species, individual stimuli fuse to yield a maximum force, known as tetanus. Similar to native muscle, engineered muscles usually exhibit positive force-frequency relationship; however, the tetanus is usually achieved at lower frequencies (10–40 Hz), most likely due to a slower  $\text{Ca}^{2+}$  transient relaxation in engineered compared to native myofibers. Similarly, relatively immature  $\text{Ca}^{2+}$  handling in engineered muscle may contribute to its lower tetanus-to-twitch ratio of  $\sim 1.5:4$ ,<sup>27,28,51,53</sup> compared to that measured in native adult muscles ( $\sim 4-10$ )<sup>48-50,52</sup> (Table 1).

Contractile forces in engineered muscles have been measured with myotubes attached to a cantilever,<sup>96</sup> small engineered muscle bundles attached to elastic posts,<sup>97</sup> and cell sheets cultured on deformable polymer sheets.<sup>98</sup> Forces as high as  $1.68 \pm 0.32$  mN for twitch and  $2.8 \pm 0.5$  mN for tetanus have been obtained for fibrin-Matrigel bundles seeded with neonatal rat myoblasts<sup>28</sup> and recently for collagen-Matrigel bundles seeded with adult mouse myoblasts.<sup>51</sup> Corresponding twitch- and tetanus-specific forces (force/cross-sectional area) in fibrin bundles were  $5.5 \pm 0.6$  kPa and  $9.4 \pm 0.7$  kPa, respectively.<sup>28</sup> Highest specific forces of  $36.3 \pm 4.2$  kPa were reported for fibrin gel-based engineered small diameter muscle bundles, made using methods similar to those of preparation of scaffold-free myooids.<sup>27</sup> By preparing fibrin hydrogels with rodent primary myoblasts that were cast around polydimethylsiloxane posts of different sizes, the forces of the resulting muscle tissues increased due to increased myofiber alignment, increased numbers of nuclei per fiber, and increased total volume occupied by myofibers.<sup>99</sup> Furthermore, engineered muscles derived from primary cells produce higher specific forces than those derived from cell lines,<sup>5</sup> suggesting important roles of non-muscle cells in the formation and functional maturation of engineered myofibers.<sup>100</sup> Additionally, not only passive but also active force generation in fibrin-based muscle bundles strongly depended on hydrogel matrix composition, revealing that similar to their roles in series-fibered muscles,<sup>101,102</sup> cell-matrix interactions may play significant roles in contractile force transmission in engineered muscle.<sup>28</sup>

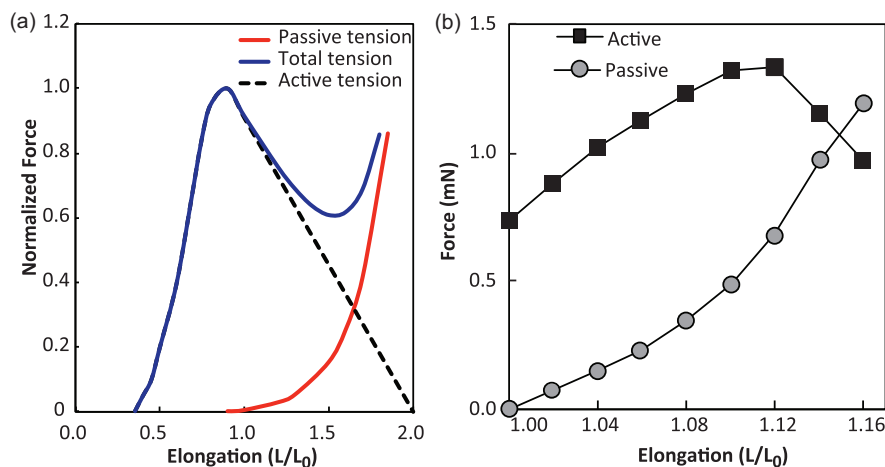


**Figure 2** Skeletal muscle dynamics (a) Force-length relationship for whole muscle showing active, passive and total tension generated. Adapted from Hall<sup>1</sup> and Bottinelli et al.<sup>95</sup> (b) Force-length relationship for rat myotubes in a fibrin gel. (A color version of this figure is available in the online journal.)

As previously noted, specific contractile (active) forces produced by engineered rodent muscles are 10–100 times less than values measured for native adult muscles *in vivo* (Table 1). A number of factors may be responsible for the lower forces *in vitro* including inadequate myofiber density and orientation, presence of fetal forms of myosin, and/or inefficient force transmission from myofibers to extracellular matrix. Increasing the initial cell density and alignment of the myoblasts may enhance the fusion of myofibers and resulting specific force.<sup>99</sup> Still, the inadequate maturation of myofibers is probably the major factor contributing to lower specific forces *in vitro* than *in vivo*. The low specific force of individual myofibers estimated from studies with small bundles of rodent muscle cells ( $0.69 \pm 0.13$  kPa),<sup>97</sup> individual myotubes on cantilevers (0.94 kPa),<sup>96</sup> and from 3D aligned muscle bundles ( $0.80 \pm 0.15$  kPa)<sup>99</sup> suggests that engineered muscles are failing to reproduce the differentiated state found *in vivo*. The relative amount of hydrogel and cells and the elastic modulus of the hydrogel influence the contribution of the passive force (Figure 2(b)) and the maximum contractile force produced is reduced as the elastic modulus of the hydrogel increases.<sup>28</sup> Thus, the cell density and elastic modulus need to be finely regulated to provide structural support for the muscle fibers to mature and develop connections with the matrix, but must not be too abundant or stiff to resist contraction.

## Methods to increase muscle maturity and force production

While engineered rat or mouse muscle tissues spontaneously contract and can produce significant contractile forces, application of electrical stimulation,<sup>26,103</sup> mechanical stimulation,<sup>26,104–106</sup> or co-culture with neurons enhance and can promote their differentiation as well as induce active contractions of muscle fibers.<sup>107,108</sup> Denervation of native muscle reduces its contractility *in vivo*,<sup>109</sup> and it is therefore expected that contractile force generation is increased by neuronal-muscle co-cultures,<sup>7</sup> or addition of a re-combinant form of agrin, a proteoglycan found in neuromuscular junctions.<sup>110</sup>

## Mechanical and electrical stimulation

Applying 17% stretch at 1 Hz on murine myoblasts<sup>111</sup> or 10% stretch at 0.5 Hz for 1 h on bovine myoblasts inhibited differentiation and promoted proliferation, while 10% strain at 0.5 Hz for 1 h alternated with 5 h of relaxation enhanced expression of integrin  $\beta_{1D}$ , which activates RhoA, thereby regulating myofiber formation, differentiation and nitric oxide release.<sup>112</sup> Cyclic stretch of engineered 3D human muscle bundles in collagen increases the construct elastic modulus and myofiber diameter.<sup>25</sup> Specifically, stimulated human muscle bundles require forces between 500 and 1000  $\mu\text{N}/10^6$  cells to stretch 15%, two to four times greater than unstretched samples.<sup>25</sup> Similarly, mechanical preconditioning of acellular porcine bladder re-populated with human skeletal myoblasts and collagen improved tissue organization and fiber orientation.<sup>108</sup> On the other hand, passive forces in collagen-

based human muscle constructs without Matrigel or mechanical stimulation are much lower with a peak force of  $43 \mu\text{N}/10^6$  cells.<sup>113</sup> In another study, human skeletal muscle constructs exhibited KCl-induced contraction after three weeks of mechanical conditioning,<sup>108</sup> although this must be interpreted cautiously since myofibroblasts also contract in response to KCl. After implantation in the mouse *latissimus dorsi* for two or three weeks, these mechanically conditioned muscle constructs exhibited tetanus, although the specific force amplitudes were far below those in the native mouse muscles, and the contribution of host versus donor cells to generated force of explanted muscle constructs was not determined.<sup>108</sup>

The beneficial effects of electrical stimulation on engineered muscle maturation and function have been shown in several studies. Low frequency electrical stimulation induced spontaneous contraction of human skeletal myofibers in 2D cultures.<sup>114</sup> Similar to exercise, low frequency stimulation of human myofibers *in vitro* increased glucose uptake independent of insulin and increased mitochondrial content and peroxisome proliferator-activated receptor gamma coactivator 1-alpha (PGC-1 $\alpha$ ) gene expression.<sup>114</sup> In murine systems, electrical stimulation rapidly produces more mature sarcomeres<sup>115</sup> as well as a higher percentage of myotubes expressing adult versus fetal MHC than fetal forms.<sup>31</sup> Electrical stimulation also promotes GLUT4 transport to the cell membrane, but does not alter the levels of GLUT1 and GLUT4.<sup>115</sup> GLUT4 activity is associated with Type I fibers that utilize oxidative metabolism compared to glycolysis.<sup>116</sup>

## Innervation

Decline in skeletal muscle function with age in humans is due, in part, to the inability of skeletal muscle to properly re-innervate with age.<sup>109</sup> Similarly, innervation of skeletal muscle *in vitro* significantly enhances functionality and increases expression of adult versus fetal isoforms of MHC.<sup>7</sup> Larkin et al.<sup>7</sup> showed that engineered 3D myooids from fetal rat skeletal myoblasts are capable of contraction 16–18 days after construct formation. Introduction of neural cells into the myooid resulted in the formation of neuromuscular-like junctions and maximal tetanus forces over two times greater than measured in aneural myooids.<sup>7</sup> Similarly, human myofibers were found to spontaneously contract only when co-cultured with human motoneurons.<sup>107</sup>

## MicroRNAs

MicroRNAs are short (~22nt), highly conserved, non-coding RNAs<sup>32,117,118</sup> that act by negatively regulating gene expression, and are usually repressors of repressors.<sup>118</sup> MicroRNAs inhibit protein translation or enhance messenger RNA degradation.<sup>119</sup> Three muscle-specific miRNA's are essential to the proliferation and differentiation of skeletal myoblasts: miR-1, miR-133a, and miR-206.<sup>32,117,118,120</sup> Specifically, miR-1 and miR-206 promote myoblast differentiation, and miR-133a promotes myoblast proliferation (Figure 3).

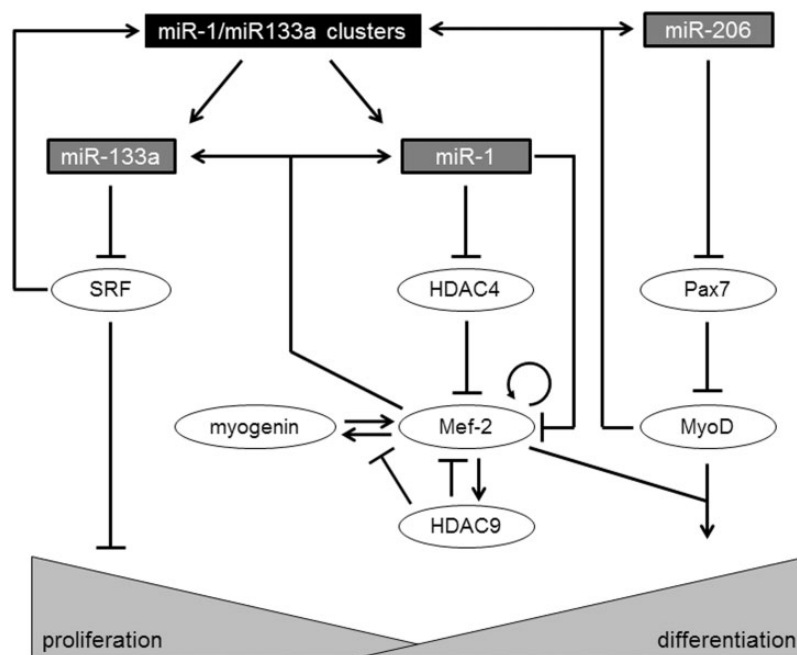


**Figure 3** Role of miR-1, miR-133a, and miR-206 in skeletal muscle proliferation and differentiation.<sup>119</sup> MiR-1 and miR-133a reside on the same gene, but they control opposing processes. MiR-133a is an inhibitor of serum response factor (SRF), which represses proliferation. MiR-1 represses histone deacetylase-4 (HDAC4), which inhibits myocyte enhancer factor-2 (Mef-2), a promoter of myoblast differentiation. The Mef-2 family of transcription factors is utilized across many different pathways; therefore, expression may vary depending on other biological stimuli. MiR-206 inhibits Pax7, which, in turn, represses MyoD expression, a marker of cell differentiation. Generally, miR-133a promotes myoblast proliferation, and miR-1/miR-206 promote myoblast differentiation

Aside from affecting muscle maturation and differentiation, microRNAs also play important roles in muscle cell metabolism<sup>121</sup> and regulation of mitochondrial biogenesis.<sup>122,123</sup> In the human and mouse genomes, miR-1 and miR-206 promote myoblast differentiation, while miR133a promotes proliferation (Figure 3). Since miR-1 and miR-133a are located on the same genetic locus, their expression is coupled, although they regulate opposing processes.<sup>118</sup> MiR-1 blocks histone deacetylase-4 (HDAC4), which inhibits myocyte enhancer factor-2 (Mef-2), transcription factors that encode proteins that promote a wide variety of muscle-specific developmental processes<sup>124</sup> including control of myoblast differentiation and function,<sup>125,126</sup> and affects the downstream metabolic co-activator PGC-1 $\alpha$  (Figure 4). A rise in Mef-2 expression is linked strongly to the onset of skeletal muscle differentiation. MiR-206 negatively affects Pax7 which leads to the promotion of MyoD, another transcription factor important to the onset and succession of muscle differentiation. MiR-696 regulates the myoblast response to mechanical stretch and affects the downstream metabolic co-activator PGC-1 $\alpha$ .<sup>127</sup>

To examine whether muscle-specific microRNA inhibitors (anti-miRs) modulate muscle function, 3D engineered muscle bundles using C2C12 myoblasts were transiently transfected with a miR-133 inhibitor (anti-miR-133) or a scrambled sequence (negative control)<sup>32</sup> leading to increased Mef-2C staining in anti-miR-133a samples compared to negative control; this indicated accelerated myoblast differentiation with inhibition of miR-133a. Additionally, miR-133a inhibition led to increased C2C12 bundle functional force output by 20% compared to

transfected control.<sup>32</sup> Anti-miR-133 transfected engineered muscle bundles contained more organized fibers, increased staining for Mef-2, and larger fiber diameters compared to negative control bundles. In 2D primary human skeletal muscle cultures, miR-133a inhibition led to increased development of striations and more sarcomeric  $\alpha$ -actinin expression six days after onset of differentiation.<sup>14</sup>

In another study, transfections of human myoblasts with miR-1 and miR-206 led to a 10-fold upregulation of miR's and accelerated differentiation, as measured by an increase in nuclear staining for MyoD and expression of  $\alpha$ -actin and myosin in 2D and 3D cultures.<sup>13</sup> These limited studies do show the promise of microRNAs or their antagonists to regulate the process of myoblast proliferation and differentiation and promote function of 3D engineered muscle tissues.

### Future challenges to reproduce human skeletal muscle physiology in 3D engineering muscle bundles

3D engineered skeletal muscle tissues mimic many of the important features of skeletal muscle *in vivo*. For example, engineered myotubes exhibit many of the key functional proteins found in mature muscle, show abundant striations, contract in response to electrical and neural stimuli, and exhibit force-length and force-frequency relationships similar to those of native muscle fibers. Some of the main limitations of these *in vitro* muscle models are that the specific forces are substantially below those found *in vivo*, immature forms of muscle proteins are present, the



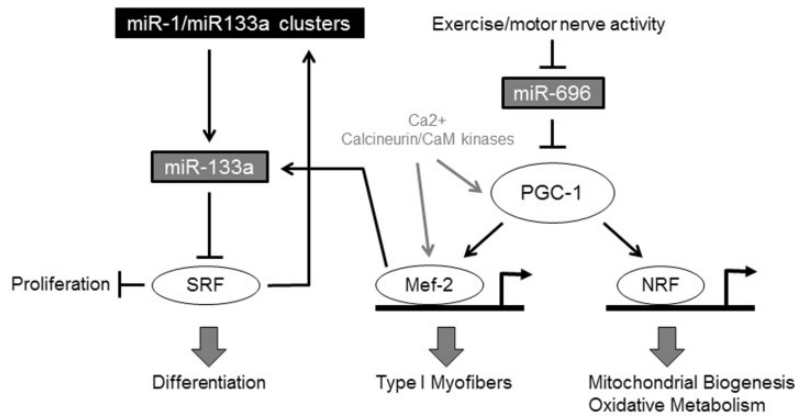


**Figure 4** Interaction of metabolic pathway with muscle differentiation. MiR-696 is downregulated with exercise and motor nerve activity, which leads to an increase in peroxisome proliferator-activated receptor gamma coactivator 1 (PGC-1), a potent transcriptional coactivator that regulates genes involved in energy metabolism. PGC-1 increases Myocyte enhancer factor-2 (Mef-2) and nuclear respiratory factor (NRF), leading to increased Type I myofiber formation and mitochondrial biogenesis/oxidative metabolism, respectively. The miR-696 pathway interacts with the previously described miR-133a pathway by way of Mef-2.<sup>127</sup>

abundance and distribution of glucose transporters *in vitro* is very different from those *in vivo*, and oxygen metabolism *in vitro* is dominated by anaerobic glycolysis, even when the muscle is relaxed.

Over the past decade, considerable advances have been made to produce 3D engineered muscle bundles with higher myofiber density. While this has been partially achieved by decreasing muscle bundle size, oxygen transport within engineered muscle still presents challenges. Novel methods to develop capillary networks are expected to enable sufficient nutrient and oxygen delivery after implantation.<sup>91</sup> Another challenge is lack of methods to regulate the fiber type, ensuring that mature fibers are produced and that conditions are developed to specifically generate Type I, IIA, or IIX fibers. Mimicking roles of innervation, either through co-culture with nerve cells or electrical stimulation and/or addition of neurotrophic factors, may be essential to producing mature human muscle fiber types. A large parameter space still needs to be explored with electrical stimulation alone or combined with mechanical stimulation. MicroRNAs provide a promising way to enhance myogenesis and function, and when expressed transiently by delivery via liposomes, could separately regulate and stimulate steps in proliferation and differentiation. In addition, methods to promote engineered muscle maturation can also be used to regulate their metabolism by altering the localization and abundance of GLUT4, PGC-1 $\alpha$  levels, and the maturity of mitochondria.

An important immediate application of functional human-engineered muscle is in predictive drug and toxicity testing *in vitro*. For this goal, however, optimized culture conditions to efficiently expand human satellite cells and myoblasts and promote their fusion and maturation need to be established. While satellite cells or purified subpopulations of muscle progenitor cells are the most likely source of cells in the near future, expanding and differentiating the cells in sufficient numbers from donors suffering from genetic or metabolic diseases will still be challenging.<sup>17</sup> On a

longer term, improved methods for myogenic differentiation of iPS cells or direct reprogramming will be required to provide sufficient numbers of cells for therapeutic applications.

**Author contributions:** All authors contributed to the writing of this manuscript. All approved the final version for submission.

#### ACKNOWLEDGEMENTS

The work was supported by grants R01AR055226 and R01AR065873 (to NB), R21AR055195 (to GAT), NSF GRFP DGE: 1106401 (to BNJD), UH2TR000505 and the NIH Common Fund for the Microphysiological Systems Initiative.

#### REFERENCES

- Hall JE. *Textbook of medical physiology*, 12th ed. Philadelphia: Saunders Elsevier, 2011
- Krans JL. The sliding filament theory of muscle contraction. *Nat Educ* 2010;3:66-9
- Rhim C, Lowell DA, Reedy MC, Slentz DH, Zhang SJ, Kraus WE, Truskey GA. Morphology and ultrastructure of differentiating three-dimensional mammalian skeletal muscle in a collagen gel. *Muscle Nerve* 2007;36:71-80
- Paul AC, Sheard PW, Kaufman SJ, Duxson MJ. Localization of alpha 7 integrins and dystrophin suggests potential for both lateral and longitudinal transmission of tension in large mammalian muscles. *Cell Tissue Res* 2002;308:255-65
- Dennis RG, Kosnik PE. Excitability and isometric contractile properties of mammalian skeletal muscle constructs engineered *in vitro*. *In Vitro Cell Dev Biol Anim* 2000;36:327-35
- Dennis RG, Kosnik PE, Gilbert ME, Faulkner JA. Excitability and contractility of skeletal muscle engineered from primary cultures and cell lines. *Am J Physiol Cell Physiol* 2001;280:C288-95
- Larkin LM, Van der Meulen JH, Dennis RG, Kennedy JB. Functional evaluation of nerve-skeletal muscle constructs engineered *in vitro*. *In Vitro Cell Dev Biol Anim* 2006;42:75-82
- Baker EL, Dennis RG, Larkin LM. Glucose transporter content and glucose uptake in skeletal muscle constructs engineered *in vitro*. *In Vitro Cell Dev Biol Anim* 2003;39:434-9
- Yin H, Price F, Rudnicki MA. Satellite cells and the muscle stem cell niche. *Physiol Rev* 2013;93:23-67

10. Cosgrove BD, Sacco A, Gilbert PM, Blau HM. A home away from home: challenges and opportunities in engineering *in vitro* muscle satellite cell niches. *Differentiation* 2009;**78**:185–94
11. Tidball JG, Villalta SA. Regulatory interactions between muscle and the immune system during muscle regeneration. *Am J Physiol Regul Integr Comp Physiol* 2010;**298**:R1173–87
12. Martin NR, Passey SL, Player DJ, Khodabukus A, Ferguson RA, Sharples AP, Mudera V, Baar K, Lewis MP. Factors affecting the structure and maturation of human tissue engineered skeletal muscle. *Biomaterials* 2013;**34**:5759–65
13. Koning M, Werker PM, Van der Schaft DW, Bank RA, Harmsen MC. MicroRNA-1 and microRNA-206 improve differentiation potential of human satellite cells: a novel approach for tissue engineering of skeletal muscle. *Tissue Eng Part A* 2012;**18**:889–98
14. Cheng CS, El-Abd Y, Bui K, Hyun YE, Hughes RH, Kraus WE, Truskey GA. Conditions that promote primary human skeletal myoblast culture and muscle differentiation *in vitro*. *Am J Physiol* 2014;**306**:C385–95
15. Aas V, Bakke S, Feng Y, Kase E, Jensen J, Bajpeyi S, Thoresen GH, Rustan A. Are cultured human myotubes far from home? *Cell Tissue Res* 2013;**354**:671–82
16. Xu C, Tabebordbar M, Salvatore Iovino S, Ciarlo C, Liu J, Castiglioni A, Price E, Min Liu M, Barton ER, Kahn CR, Wagers AJ, Zon LI. A zebrafish embryo culture system defines factors that promote vertebrate myogenesis across species. *Cell* 2013;**155**:909–21
17. Fishman JM, Tyraskis A, Maghsoudlou P, Urbani L, Totonelli G, Birchall MA, De Coppi P. Skeletal muscle tissue engineering: which cell to use? *Tissue Eng Part B: Rev* 2013;**19**:503–15
18. Usas A, Huard J. Muscle-derived stem cells for tissue engineering and regenerative therapy. *Biomaterials* 2007;**28**:5401–6
19. Li H, Usas A, Poddar M, Chen C-W, Thompson S, Ahani B, Cummins J, Lavasani M, Huard J. Platelet-rich plasma promotes the proliferation of human muscle derived progenitor cells and maintains their stemness. *PLoS One* 2013;**8**:e64923
20. Vella JB, Thompson SD, Bucsek MJ, Song M, Huard J. Murine and human myogenic cells identified by elevated aldehyde dehydrogenase activity: implications for muscle regeneration and repair. *PLoS One* 2011;**6**:e29226
21. Xu C, Tabebordbar M, Iovino S, Ciarlo C, Liu J, Castiglioni A, Price E, Liu M, Barton ER, Kahn CR, Wagers AJ, Zon LI. A zebrafish embryo culture system defines factors that promote vertebrate myogenesis across species. *Cell* 2013;**155**:909–21
22. Darabi R, Arpke RW, Irion S, Dimos JT, Grskovic M, Kyba M, Perlingeiro RCR. Human ES- and iPS-derived myogenic progenitors restore DYSTROPHIN and improve contractility upon transplantation in dystrophic mice. *Cell Stem Cell* 2012;**10**:610–9
23. Borchin B, Chen J, Barberi T. Derivation and FACS-mediated purification of pax3+/pax7+ skeletal muscle precursors from human pluripotent stem cells. *Stem Cell Rep* 2013;**1**:620–31
24. Riboldi SA, Sadr N, Pignini L, Neuenschwander P, Simonet M, Mognol P, Sampaolesi M, Cossu G, Mantero S. Skeletal myogenesis on highly orientated microfibrillar polyurethane scaffolds. *J Biomed Mater Res A* 2008;**84**:1094–101
25. Powell CA, Smiley BL, Mills J, Vandeburgh HH. Mechanical stimulation improves tissue-engineered human skeletal muscle. *Am J Physiol Cell Physiol* 2002;**283**:C1557–65
26. Liao IC, Liu JB, Bursac N, Leong KW. Effect of electromechanical stimulation on the maturation of myotubes on aligned electrospun fibers. *Cell Mol Bioeng* 2008;**1**:133–45
27. Huang Y-C, Dennis RG, Larkin L, Baar K. Rapid formation of functional muscle *in vitro* using fibrin gels. *J Appl Physiol* 2005;**98**:706–13
28. Hinds S, Bian W, Dennis RG, Bursac N. The role of extracellular matrix composition in structure and function of bioengineered skeletal muscle. *Biomaterials* 2011;**32**:3575–83
29. Aubin H, Nichol JW, Hutson CB, Bae H, Sieminski AL, Cropek DM, Akhyari P, Khademhosseini A. Directed 3D cell alignment and elongation in microengineered hydrogels. *Biomaterials* 2010;**31**:327–35
30. Gillies AR, Lieber RL. Structure and function of the skeletal muscle extracellular matrix. *Muscle Nerve* 2011;**44**:318–31
31. Langelaan MPL, Boonen KJM, Rosaria-Chak KY, Van der Schaft DWJ, Mark J, Post MJ, Baaijens FPT. Advanced maturation by electrical stimulation: differences in response between C2C12 and primary muscle progenitor cells. *J Tissue Eng Regen Med* 2011;**5**:529–39
32. Rhim C, Cheng CS, Kraus WE, Truskey GA. Effect of microRNA modulation on bioartificial muscle function. *Tissue Eng Part A* 2010;**16**(12): 3589–97
33. Janmey PA, Winer JP, Weisel JW. Fibrin gels and their clinical and bioengineering applications. *J R Soc Interface* 2009;**6**:1–10
34. Engler AJ, Griffin MA, Sen S, Bönnemann CG, Sweeney HL, Discher DE. Myotubes differentiate optimally on substrates with tissue-like stiffness: pathological implications for soft or stiff microenvironments. *J Cell Biol* 2004;**166**:877–87
35. Discher DE, Janmey P, Wang Y-I. Tissue cells feel and respond to the stiffness of their substrate. *Science* 2005;**310**:1139–43
36. Chopra A, Lin V, McCollough A, Atzet S, Prestwich GD, Wechsler AS, Murray ME, Oake SA, Kresh JY, Janmey PA. Reprogramming cardiomyocyte mechanosensing by crosstalk between integrins and hyaluronic acid receptors. *J Biomech* 2012;**45**:824–41
37. Chaudhuri O, Mooney DJ. Stem-cell differentiation: anchoring cell-fate cues. *Nat Mater* 2012;**11**:568–9
38. Saltiel AR, Kahn CR. Insulin signalling and the regulation of glucose and lipid metabolism. *Nature* 2001;**414**:799–806
39. Barnard RJ, Youngren JF. Regulation of glucose transport in skeletal muscle. *FASEB J* 1992;**6**:3238–44
40. Scott W, Stevens J, Binder-MacLeod SA. Human skeletal muscle fiber type classifications. *Phys Ther* 2001;**81**:1810–6
41. Schiaffino S, Reggiani C. Fiber types in mammalian skeletal muscles. *Physiol Rev* 2011;**91**:1447–531
42. Agbulut O, Noirez P, Beaumont F, Butler-Browne G. Myosin heavy chain isoforms in postnatal muscle development of mice. *Biol Cell* 2003;**95**:399–406
43. Galpin AJ, Raue U, Jemiolo B, Trappe TA, Harber MP, Minchev K, Trappe S. Human skeletal muscle fiber type specific protein content. *Anal Biochem* 2012;**425**:175–82
44. Greising SM, Gransee HM, Mantilla CB, Sieck GC. Systems biology of skeletal muscle: fiber type as an organizing principle. *Wiley Interdiscip Rev Syst Biol Med* 2012;**4**:457–73
45. Costford SR, Kavaslar N, Ahituv N, Chaudhry SN, Schackwitz WS, Dent R, Pennacchio LA, McPherson R, Harper ME. Gain-of-function R225W mutation in human AMPKgamma(3) causing increased glyco-gen and decreased triglyceride in skeletal muscle. *PLoS One* 2007;**2**:e903
46. Vandeburgh H, Shansky J, Benesch-Lee F, Barbata V, Reid J, Thorrez L, Valentini R, Crawford G. Drug-screening platform based on the contractility of tissue-engineered muscle. *Muscle Nerve* 2008;**37**:438–47
47. Bloemberg D, Quadrilatero J. Rapid determination of myosin heavy chain expression in rat, mouse, and human skeletal muscle using multicolor immunofluorescence analysis. *PLoS One* 2012;**7**:e35273
48. Pistilli EE, Bogdanovich S, Garton F, Yang N, Gulbin JP, Conner JD, Anderson BG, Quinn LS, North K, Ahima RS, Khurana TS. Loss of IL-15 receptor  $\alpha$  alters the endurance, fatigability, and metabolic characteristics of mouse fast skeletal muscles. *J Clin Invest* 2011;**121**:3120–32
49. Gagnon M, Maguire M, MacDermott M, Bradford A. Effects of creatine loading and depletion on rat skeletal muscle contraction. *Clin Exp Pharmacol Physiol* 2002;**29**:885–90
50. Celichowski J, Grottel K. Twitch/tetanus ratio and its relation to other properties of motor units. *Neuroreport* 1993;**13**:201–4
51. Lee PHU, Vandeburgh HH. Skeletal muscle atrophy in bioengineered skeletal muscle: a new model system. *Tissue Eng Part A* 2013;**19**:2147–55
52. Seki K, Taniguchi Y, Narusawa M. Alterations in contractile properties of human skeletal muscle induced by joint immobilization. *J Physiol* 2001;**530**:521–32
53. Carosio S, Barberi L, Rizzuto E, Nicoletti C, Prete ZD, Musarò A. Generation of eX vivo-vascularized Muscle Engineered Tissue (X-MET). *Sci Rep* 2013;**3**:1420
54. Maganaris CN, Baltzopoulos V, Ball D, Sargeant AJ. *In vivo* specific tension of human skeletal muscle. *J Appl Physiol* 1985;**90**:865–72
55. Huang YC, Dennis RG, Larkin L, Baar K. Rapid formation of functional muscle *in vitro* using fibrin gels. *J Appl Physiol* 1985;**98**:706–13

56. Brooks SV. Rapid recovery following contraction-induced injury to in situ skeletal muscles in mdx mice. *J Muscle Res Cell Motil* 1998;**19**:179–87
57. Urbanek MG, Picken EB, Kalliainen LK, Kuzon WM Jr. Specific force deficit in skeletal muscles of old rats is partially explained by the existence of denervated muscle fibers. *J Gerontol A Biol Sci Med Sci* 2001;**56**:B191–7
58. Dennis RG, Kosnik PE 2nd, Gilbert ME, Faulkner JA. Excitability and contractility of skeletal muscle engineered from primary cultures and cell lines. *Am J Physiol Cell Physiol* 2001;**280**:C288–95
59. Vandenburg HH, Swadison S, Karlisch P. Computer-aided mechanogenesis of skeletal muscle organs from single cells *in vitro*. *Faseb J* 1991;**5**:2860–7
60. LeBrasseur NK, Walsh K, Arany Z. Metabolic benefits of resistance training and fast glycolytic skeletal muscle. *Am J Physiol Endocrinol Metab* 2011;**300**:2
61. Van Wessel T, De Haan A, Van der Laarse WJ, Jaspers RT. The muscle fiber type-fiber size paradox: hypertrophy or oxidative metabolism? *Eur J Appl Physiol* 2010;**110**:665–94
62. Van Beekvelt MC, Colier WN, Wevers RA, Van Engelen BG. Performance of near-infrared spectroscopy in measuring local O<sub>2</sub> consumption and blood flow in skeletal muscle. *J Appl Physiol* 2001;**90**:511–9
63. De Blasi RA, Ferrari M, Natali A, Conti G, Mega A, Gasparetto A. Noninvasive measurement of forearm blood flow and oxygen consumption by near-infrared spectroscopy. *J Appl Physiol* 1994;**76**:1388–93
64. Zelis R, Longhurst J, Capone RJ, Mason DT. A comparison of regional blood flow and oxygen utilization during dynamic forearm exercise in normal subjects and patients with congestive heart failure. *Circulation* 1974;**50**(1): 137–43
65. Mottram RF. The oxygen consumption of human skeletal muscle *in vivo*. *J Physiol* 1955;**128**:268–76
66. Gurley K, Shang Y, Yu G. Noninvasive optical quantification of absolute blood flow, blood oxygenation, and oxygen consumption rate in exercising skeletal muscle. *J Biomed Opt* 2012;**17**:075010
67. Blomstrand E, Radegran G, Saltin B. Maximum rate of oxygen uptake by human skeletal muscle in relation to maximal activities of enzymes in the Krebs cycle. *J Physiol* 1997;**501**(Pt 2): 455–60
68. Mehta G, Mehta K, Sud D, Song JW, Bersano-Begey T, Futai N, Heo YS, Mycek MA, Linderman JJ, Takayama S. Quantitative measurement and control of oxygen levels in microfluidic poly(dimethylsiloxane) bioreactors during cell culture. *Biomed Microdevices* 2007;**9**:123–34
69. Guarino RD, Dike LE, Haq TA, Rowley JA, Pitner JB, Timmins MR. Method for determining oxygen consumption rates of static cultures from microplate measurements of pericellular dissolved oxygen concentration. *Biotechnol Bioeng* 2004;**86**:775–87
70. Feige JN, Lagouge M, Canto C, Strehle A, Houten SM, Milne JC, Lambert PD, Matakis C, Elliott PJ, Auwerx J. Specific SIRT1 activation mimics low energy levels and protects against diet-induced metabolic disorders by enhancing fat oxidation. *Cell Metab* 2008;**8**:347–58
71. Minners J, Lacerda L, McCarthy J, Meiring JJ, Yellon DM, Sack MN. Ischemic and pharmacological preconditioning in girardi cells and C2C12 myotubes induce mitochondrial uncoupling. *Circ Res* 2001;**89**:787–92
72. Sun X, Zemel MB. Leucine modulation of mitochondrial mass and oxygen consumption in skeletal muscle cells and adipocytes. *Nutr Metab* 2009;**6**:26–33
73. Kinsey ST, Locke BR, Dillaman RM. Molecules in motion: influences of diffusion on metabolic structure and function in skeletal muscle. *J Exp Biol* 2011;**214**(Pt 2): 263–74
74. Karande TS, Ong JL, Agrawal CM. Diffusion in musculoskeletal tissue engineering scaffolds: design issues related to porosity, permeability, architecture, and nutrient mixing. *Ann Biomed Eng* 2004;**32**(12): 1728–43
75. Ishaug SL, Crane GM, Miller MJ, Yasko AW, Yaszemski MJ, Mikos AG. Bone formation by three-dimensional stromal osteoblast culture in biodegradable polymer scaffolds. *J Biomed Mater Res* 1997;**36**:17–28
76. Muschler GF, Nakamoto C, Griffith LG. Engineering principles of clinical cell-based tissue engineering. *J Bone Joint Surg Am* 2004;**86**:1541–58
77. Di Carlo A, De Mori R, Martelli F, Pompilio G, Capogrossi MC, Germani A. Hypoxia inhibits myogenic differentiation through accelerated MyoD degradation. *J Biol Chem* 2004;**279**:16332–8
78. Yun Z, Lin Q, Giaccia AJ. Adaptive myogenesis under hypoxia. *Mol Cell Biol* 2005;**25**:3040–55
79. Chakravarthy MV, Spangenburg EE, Booth FW. Culture in low levels of oxygen enhances *in vitro* proliferation potential of satellite cells from old skeletal muscles. *Cell Mol Life Sci* 2001;**58**:1150–8
80. Csete M, Walikonis J, Slawny N, Wei Y, Korsnes S, Doyle JC, Wold B. Oxygen-mediated regulation of skeletal muscle satellite cell proliferation and adipogenesis in culture. *J Cell Physiol* 2001;**189**:189–96
81. Kook SH, Son YO, Lee KY, Lee HJ, Chung WT, Choi KC, Lee JC. Hypoxia affects positively the proliferation of bovine satellite cells and their myogenic differentiation through up-regulation of MyoD. *Cell Biol Int* 2008;**32**:871–8
82. Martin SD, Collier FM, Kirkland MA, Walder K, Stupka N. Enhanced proliferation of human skeletal muscle precursor cells derived from elderly donors cultured in estimated physiological (5%) oxygen. *Cytotechnology* 2009;**61**:93–107
83. Redshaw Z, Loughna PT. Oxygen concentration modulates the differentiation of muscle stem cells toward myogenic and adipogenic fates. *Differentiation* 2012;**84**:193–202
84. Koning M, Werker PM, Van Luyn MJ, Harmsen MC. Hypoxia promotes proliferation of human myogenic satellite cells: a potential benefactor in tissue engineering of skeletal muscle. *Tissue Eng Part A* 2011;**17**:1747–58
85. Stamati K, Mudera V, Cheema U. Evolution of oxygen utilization in multicellular organisms and implications for cell signalling in tissue engineering. *J Tissue Eng* 2011;**2**:16
86. Chromiak JA, Shansky J, Perrone C, Vandenburg HH. Bioreactor perfusion system for the long-term maintenance of tissue-engineered skeletal muscle organoids. *In Vitro Cell Dev Biol Anim* 1998;**34**:694–703
87. Fujita H, Shimizu K, Morioka Y, Nagamori E. Enhancement of C2C12 differentiation by perfluorocarbon-mediated oxygen delivery. *J Biosci Bioeng* 2010;**110**:359–262
88. Sato M, Ito A, Akiyama H, Kawabe Y, Kamihira M. Effects of B-cell lymphoma 2 gene transfer to myoblast cells on skeletal muscle tissue formation using magnetic force-based tissue engineering. *Tissue Eng Part A* 2013;**19**:307–15
89. Koffler J, Kaufman-Francis K, Shandalov Y, Egozi D, Amiad Pavlov D, Landesberg A, Levenberg S. Improved vascular organization enhances functional integration of engineered skeletal muscle grafts. *Proc Natl Acad Sci* 2011;**108**:14789–94
90. Auger FA, Gibot L, Lacroix D. The pivotal role of vascularization in tissue engineering. *Annu Rev Biomed Eng* 2013;**15**:177–200
91. Serbo JV, Gerecht S. Vascular tissue engineering: biodegradable scaffold platforms to promote angiogenesis. *Stem Cell Res Ther* 2013;**4**:8
92. Au P, Tam J, Fukumura D, Jain RK. Bone marrow-derived mesenchymal stem cells facilitate engineering of long-lasting functional vasculature. *Blood* 2008;**111**:4551–8
93. Sasagawa T, Shimizu T, Sekiya S, Haraguchi Y, Yamato M, Sawa Y, Okano T. Design of prevascularized three-dimensional cell-dense tissues using a cell sheet stacking manipulation technology. *Biomaterials* 2010;**31**:1646–54
94. Larkin LM, Calve S, Kostrominova TY, Arruda EM. Structure and functional evaluation of tendon-skeletal muscle constructs engineered *in vitro*. *Tissue Eng* 2006;**12**:3149–58
95. Bottinelli R, Canepari M, Pellegrino MA, Reggiani C. Force-velocity properties of human skeletal muscle fibres: myosin heavy chain isoform and temperature dependence. *J Physiol* 1996;**495**(Pt 2): 573–86
96. Pirozzi KL, Long CJ, McAleer CW, Smith AST, Hickman JJ. Correlation of embryonic skeletal muscle myotube physical characteristics with contractile force generation on an atomic force microscope-based biomechanical systems device. *Appl Phys Lett* 2013;**103**:083108
97. Sakar MS, Neal D, Boudou T, Borochin MA, Li Y, Weiss R, Kamm RD, Chen CS, Asada HH. Formation and optogenetic control of engineered 3D skeletal muscle bioactuators. *Lab Chip* 2012;**12**:4976–85
98. Sun Y, Duffy R, Lee A, Feinberg AW. Optimizing the structure and contractility of engineered skeletal muscle thin films. *Acta Biomater* 2013;**9**:7885–94

99. Bian W, Juhas M, Pfeiler TW, Bursac N. Local tissue geometry determines contractile force generation of engineered muscle networks. *Tissue Eng Part A* 2012;**18**:957–67
100. Li M, Dickinson CE, Finkelstein EB, Neville CM, Sundback CA. The role of fibroblasts in self-assembled skeletal muscle. *Tissue Eng Part A* 2011;**17**:2641–50
101. Young M, Paul A, Rodda J, Duxson M, Sheard P. Examination of intrafascicular muscle fiber terminations: implications for tension delivery in series-fibered muscles. *J Morphol* 2000;**245**:130–45
102. Paul A, Sheard P, Kaufman S, Duxson M. Localization of  $\alpha 7$  integrins and dystrophin suggests potential for both lateral and longitudinal transmission of tension in large mammalian muscles. *Cell Tissue Res* 2002;**308**:255–65
103. Donnelly K, Khodabukus A, Philp A, Deldicque L, Dennis RG, Baar K. A novel bioreactor for stimulating skeletal muscle *in vitro*. *Tissue Eng Part C Methods* 2010;**16**:711–8
104. Candiani G, Riboldi SA, Sadr N, Lorenzoni S, Neuenschwander P, Montevecchi FM, Mantero S. Cyclic mechanical stimulation favors myosin heavy chain accumulation in engineered skeletal muscle constructs. *J Appl Biomater Biomech* 2010;**8**:68–75
105. Machingal MA, Corona BT, Walters TJ, Kesireddy V, Koval CN, Dannahower A, Zhao W, Yoo JJ, Christ GJ. A tissue-engineered muscle repair construct for functional restoration of an irrecoverable muscle injury in a murine model. *Tissue Eng Part A* 2011;**17**:2291–303
106. Vandenburg HH. A computerized mechanical cell stimulator for tissue culture: effects on skeletal muscle organogenesis. *In Vitro Cell Dev Biol* 1988;**24**:609–19
107. Guo X, Gonzalez M, Stancescu M, Vandenburg HH, Hickman JJ. Neuromuscular junction formation between human stem cell-derived motoneurons and human skeletal muscle in a defined system. *Biomaterials* 2011;**32**:9602–11
108. Moon du G, Christ G, Stitzel JD, Atala A, Yoo JJ. Cyclic mechanical preconditioning improves engineered muscle contraction. *Tissue Eng Part A* 2008;**14**:473–82
109. Larkin LM, Kuzon WM, Halter JB. Effects of age and nerve-repair grafts on reinnervation and fiber type distribution of rat medial gastrocnemius muscles. *Mech Ageing Dev* 2003;**124**:653–61
110. Bian W, Bursac N. Soluble miniagrin enhances contractile function of engineered skeletal muscle. *FASEB J* 2012;**26**:955–65
111. Kumar A, Murphy R, Robinson P, Wei L, Boriek AM. Cyclic mechanical strain inhibits skeletal myogenesis through activation of focal adhesion kinase, Rac-1 GTPase, and NF-kappaB transcription factor. *FASEB J* 2004;**18**:1524–35
112. Zhang SJ, Truskey GA, Kraus WE. Effect of cyclic stretch on beta1D-integrin expression and activation of FAK and RhoA. *Am J Physiol Cell Physiol* 2007;**292**:C2057–69
113. Mudera V, Smith AS, Brady MA, Lewis MP. The effect of cell density on the maturation and contractile ability of muscle derived cells in a 3D tissue-engineered skeletal muscle model and determination of the cellular and mechanical stimuli required for the synthesis of a postural phenotype. *J Cell Physiol* 2010;**225**:646–53
114. Nikolić N, Bakke SS, Kase ET, Rudberg I, Flo Halle I, Rustan AC, Thoresen GH, Aas V. Electrical pulse stimulation of cultured human skeletal muscle cells as an *in vitro* model of exercise. *PLoS One* 2012;**7**:e33203
115. Nedachi T, Fujita H, Kanzaki M. Contractile C2C12 myotube model for studying exercise-inducible responses in skeletal muscle. *Am J Physiol* 2008;**295**:E1191–204
116. Richter EA, Hargreaves M. Exercise, GLUT4, and skeletal muscle glucose uptake. *Physiol Rev* 2013;**93**:993–1017
117. Chen JF, Tao Y, Li J, Deng Z, Yan Z, Xiao X, Wang DZ. microRNA-1 and microRNA-206 regulate skeletal muscle satellite cell proliferation and differentiation by repressing Pax7. *J Cell Biol* 2010;**190**:867–79
118. Townley-Tilson WH, Callis TE, Wang D. MicroRNAs 1, 133, and 206: critical factors of skeletal and cardiac muscle development, function, and disease. *Int J Biochem Cell Biol* 2010;**42**:1252–5
119. Guller I, Russell AP. MicroRNAs in skeletal muscle: their role and regulation in development, disease and function. *J Physiol* 2010;**588**(Pt 21): 4075–87
120. Morley JE, Perry HM 3rd, Miller DK. Editorial: Something about frailty. *J Gerontol A Biol Sci Med Sci* 2002;**57**:M698–704
121. Crist CG, Buckingham M. Megarole for microRNA in muscle disease. *Cell Metab* 2010;**12**:425–6
122. Potthoff MJ, Wu H, Arnold MA, Shelton JM, Backs J, McAnally J, Richardson JA, Bassel-Duby R, Olson EN. Histone deacetylase degradation and MEF2 activation promote the formation of slow-twitch myofibers. *J Clin Invest* 2007;**117**:2459–67
123. Wu H, Kanatous SB, Thurmond FA, Gallardo T, Isotani E, Bassel-Duby R, Williams RS. Regulation of mitochondrial biogenesis in skeletal muscle by CaMK. *Science* 2002;**296**:349–52
124. Potthoff MJ, Arnold MA, McAnally J, Richardson JA, Bassel-Duby R, Olson EN. Regulation of skeletal muscle sarcomere integrity and postnatal muscle function by Mef2c. *Mol Cell Biol* 2007;**27**:8143–51
125. Molkenin JD, Olson EN. Combinatorial control of muscle development by basic helix-loop-helix and MADS-box transcription factors. *Proc Natl Acad Sci U S A* 1996;**93**:9366–73
126. Ornatsky OI, Andreucci JJ, McDermott JC. A dominant-negative form of transcription factor MEF2 inhibits myogenesis. *J Biol Chem* 1997;**272**:33271–8
127. Aoi W, Naito Y, Mizushima K, Takanami Y, Kawai Y, Ichikawa H, Yoshikawa T. The microRNA miR-696 regulates PGC-1{alpha} in mouse skeletal muscle in response to physical activity. *Am J Physiol Endocrinol Metab* 2010;**298**:E799–806